Clays and Clay Minerals, Vol. 38, No. 3, 241–249, 1990.

CHARACTERIZATION OF ILLITIZATION OF SMECTITE IN BENTONITE BEDS AT KINNEKULLE, SWEDEN

ATSUYUKI INOUE,[1] TAKASHI WATANABE,[2] NORIHIKO KOHYAMA,[3] AND ANN MARIE BRUSEWITZ[4]

[1]Geological Institute, College of Arts and Sciences,
Chiba University, Chiba 260, Japan

[2]Johetsu University of Education, Johetsu, Niigata 943, Japan

[3]National Institute of Industrial Health, The Ministry of Labor
Nagao, Tama-ku, Kawasaki 213, Japan

[4]Geological Survey of Sweden, Box 670, S-75128 Uppsala, Sweden

Abstract—Structure, morphology, and chemical composition of illite/smectite (I/S) containing 30–50% smectite layers (% S) from Kinnekulle bentonites, Sweden, of diagenetic origin were examined using X-ray powder diffraction (XRD) and transmission electron microscopy (TEM). Interlayer arrangements of I/S changed from random interstratification to short-range ordered at about 40% S. The transition from random to ordered structure proceeded continuously as reflected by the gradual decrease in probability of two smectite neighbors (P_{ss}) towards zero. TEM observations of water-dispersed samples that had not been cation-exchanged showed that the I/S consisted dominantly of flakes coexisting with laths having a length/width ratio of about 4, regardless of % S. The thickness of the I/S particles ranged from 30 to 100 Å, and no systematic variation in thickness was detected with decreasing % S. The chemical composition of the I/S also changed continuously with decreasing % S. These observations suggest no dissolution of smectite layers and no recrystallization of illite layers during the formation of the I/S in these bentonites; rather, cationic substitutions occurred within a smectite precursor (termed a solid-state transformation mechanism). A comparison of interlayer order, particle texture, and chemistry of the I/S from various types of rocks suggests that the mechanism of smectite-to-illite conversion in the range 100% S–30% S was related to the porosity and permeability of original rocks. The solid-state transformation mechanism appears to have predominated in rocks of low porosity and permeability.

Key Words—Bentonite, Diagenesis, Illite/smectite, Illitization, Transmission electron microscopy, X-ray powder diffraction.

INTRODUCTION

The smectite-to-illite reaction has been reported to be a sensitive mineral indicator of the thermal history of rocks formed in a wide range of diagenetic to low-grade metamorphic environments (e.g., Hoffman and Hower, 1979; Inoue and Utada, 1983; Środoń and Eberl, 1984; Horton, 1985). With increasing temperature, smectite commonly converts to illite through interstratified illite/smectite (I/S) intermediate products. The ratio of illite to smectite layers and the ordering of interlayer stacking (termed Reichweite, or g, which was initially defined by Jagodzinski, 1949) change concomitantly with the conversion. The degree of illitization of smectite also appears to be influenced by the chemistry of the pore solution, the porosity and permeability of the strata, and the residence time of the strata at a given temperature (Eberl and Hower, 1976; Roberson and Lahann, 1981; Altaner *et al.*, 1984; Ramseyer and Boles, 1986; Yau *et al.*, 1987; Glasmann et al., 1989).

Two mechanisms for the smectite-to-illite conversion have been described: (1) solid-state transformation and (2) neoformation. The solid-state transformation (SST) mechanism calls for substitution of Al for Si in an intact 2:1 layer of precursor smectite and for an exchange of Na (and/or Ca) and K in the interlayer (Pollard, 1971; Hower *et al.*, 1976). This hypothesis was deduced mainly from chemical and X-ray powder diffraction (XRD) studies of I/S (e.g., Hower *et al.*, 1976). In the neoformation mechanism, the conversion proceeds via the dissolution of smectite and small illite crystallites and the recrystallization of larger illite crystallites (Nadeau *et al.*, 1984, 1985; Inoue *et al.*, 1987, 1988). Moreover, the recrystallization and growth of larger illite crystallites are controlled by an Ostwald ripening process (Inoue *et al.*, 1988; Eberl and Środoń, 1988).

A main distinction in the two mechanisms can be drawn in the behavior of precursor smectite layers during the course of conversion. In the SST process, some layers within a packet of precursor smectite layers can remain intact over nearly the entire stage of the conversion, even if other smectite layers are cannibalized, as emphasized by Boles and Franks (1979), Hower (1981), and Pollastro (1985). On the contrary, in the neoformation process all precursor smectite layers dissolve completely at an intermediate stage of the conversion. Many variants of these mechanisms exist, but they can be categorized broadly as either the SST or neoformation. Experimentally, a drastic change in morphology of I/S particles from hydrothermally altered tuffs noted by transmission electron microscopy (TEM), which occurred from flake to lath with decreas-

Table 1. Description of bentonite samples from Kinnekulle, Sweden.

Sample	Thickness (cm)	K-Ar age (Ma)	Impurities[1]
A1	15	—	kaolinite
A2	14	—	biotite, kaolinite, chlorite, quartz
B31	180	336	biotite, kaolinite, chlorite, quartz
B33		328	kaolinite, chlorite, quartz
B38		292	kaolinite, chlorite, quartz
STM6		—	kaolinite, quartz
K71	30	336	kaolinite
K74	15	317	
K78	3	338	chlorite

[1] In the <1-μm size fraction.

ing % S, strongly supported the neoformation mechanism (Inoue *et al.*, 1987). Yau *et al.* (1987) also demonstrated using TEM that neoformation was predominate in the formation of illite in shales from the Salton Sea geothermal field. Thus, the data obtained to date seem to favor the neoformation mechanism for the smectite-to-illite conversion in hydrothermal systems, although a question remains of whether I/S in hydrothermal products was really formed from a smectite precursor, as mentioned by Bethke *et al.* (1986). In contrast, ambiguities also remain in reaction mechanism in shales, sandstones, and bentonites of diagenetic origin. Glasmann *et al.* (1989) reported lath-shaped I/S in relatively coarse-grained shales from North Sea drill cores and related the existence of euhedral I/S particles to the high porosity of rocks during diagenesis.

Shales usually contain detrital illite and, therefore, detrital and authigenic I/S are not easily distinguished by TEM. Bentonites, however, seem to be more suitable for studying the mechanism of smectite-to-illite conversion, because the mineralogy of bentonite is comparatively homogeneous. In this paper, we describe interlayer ordering schemes, shape, and chemistry of I/S from Kinnekulle bentonites based on XRD and TEM investigations. A possible mechanism of the smectite-to-illite conversion in diagenetic bentonites is also discussed.

SAMPLES AND EXPERIMENTAL METHODS

Kinnekulle bentonites

Figure 1 shows a schematic section of the Kinnekulle strata. The Kinnekulle bentonite beds can generally be classified as Silurian or Ordovician beds (Brusewitz, 1986). The percentage of smectite layers (% S) in I/S from the Silurian beds is nearly constant at 5–15%. Such extensive illitization was due to the thermal effect of later diabase intrusion (about 300 Ma). The % S in I/S from the Ordovician beds ranges from 30 to 50%. The Ordovician bentonites seem to have been only weakly subjected to the thermal effect of diabase intrusion, and are essentially of diagenetic origin. In the present study, nine samples of I/S were collected from the Ordovician bentonites, A, B, and C beds (Figure 1), to avoid the thermal effect of the diabase intrusion in the smectite-to-illite conversion. The rock samples contain quartz, feldspar, biotite, chlorite, and kaolinite as impurities. Most of these phases were eliminated by decantation and centrifugation, but small amounts of kaolinite, chlorite, biotite, and quartz remained in the <1-μm fraction (Table 1). The K-Ar ages of these samples given by Brusewitz (1984, 1986) are listed in Table 1.

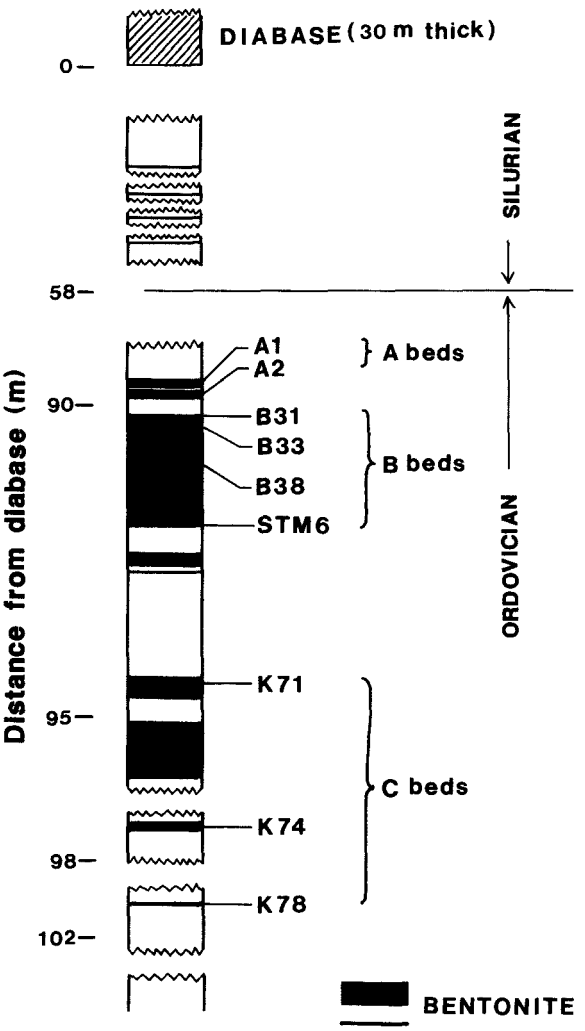

Figure 1. Schematic columnar section of Kinnekulle bentonites, indicating the position of samples used in the present study.

Experimental methods

The <1-μm fractions of the bentonites were examined by XRD and analytical and transmission electron

https://doi.org/10.1346/CCMN.1990.0380302 Published online by Cambridge University Press

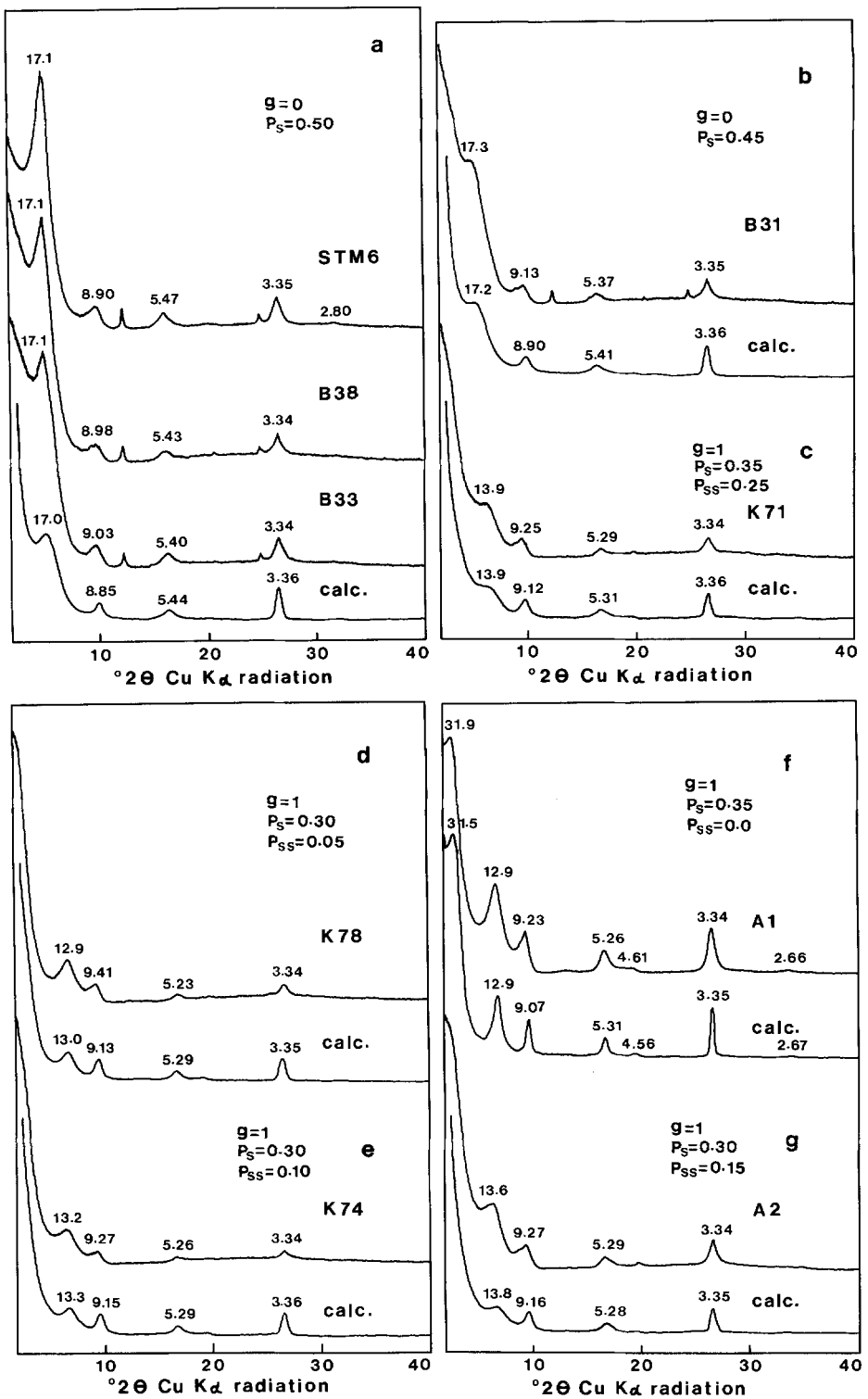

Figure 2. Comparison of observed and calculated X-ray powder diffraction patterns of ethylene glycol-saturated specimens. (a) samples STM6, B38, and B33, (b) sample B31, (c) sample K71, (d) sample K78, (e) sample K74, (f) sample A1, and (g) sample A2. Numbers indicate d-values of peaks in Ångstroms.

https://doi.org/10.1346/CCMN.1990.0380302 Published online by Cambridge University Press

Table 2. Predominant ordering, existence probabilities of smectite (P_S) and illite (P_I) layers, and transition probabilities from smectite to smectite (P_{SS}) and from illite to illite (P_{II}) for Kinnekulle bentonites.

Samples[1]	Ordering	P_S (previous data[2])	P_I	P_{SS}	P_{II}
A1	g = 1	0.35 (0.37)	0.65	0.00	0.462
A2	g = 1	0.30 (0.32–0.38)	0.70	0.15	0.636
B31	g = 0	0.45 (0.35–0.45)	0.55	0.45	0.55
B33	g = 0	0.50 (0.41–0.50)	0.50	0.50	0.50
B38	g = 0	0.50 (0.51–0.55)	0.50	0.50	0.50
STM6	g = 0	0.50 (0.52–0.60)	0.50	0.50	0.50
K71	g = 1	0.35 (0.30)	0.65	0.25	0.596
K74	g = 1	0.30 (0.30)	0.70	0.10	0.614
K78	g = 1	0.30 (0.25)	0.70	0.05	0.593

[1] See Table 1 for sample descriptions.
[2] After Hower and Mowatt (1966), Reynolds and Hower (1970), Brusewitz (1986, 1988), and Inoue *et al.* (1989).

microscopy (AEM and TEM). XRD patterns were obtained on the original samples and cation-saturated samples (e.g., Na, K, Mg, Ca, and Sr) and their air-dried and ethylene glycol (EG)-saturated specimens using a Rigaku RAD I-B diffractometer (40 kV, 20 mA) equipped with a Cu tube, a graphite monochrometer, and 0.5° divergence and scattering slits. TEM observations and elemental analyses were made on the <1-μm fractions spread on Ni TEM grids using a Hitachi H-500 transmission electron microscope equipped with a Kevex 5000 solid-state detector for energy-dispersive X-ray analysis (EDX) and a microcomputer for quantitative data processing. The thicknesses of I/S particles were measured in the TEM after Pt-Pd shadowing. The methods of TEM investigations used here followed Inoue *et al.* (1987). No chemical treatments, such as Na- or Li-exchange (Nadeau *et al.*, 1985), were performed on the TEM specimens.

Structure determination of I/S

Smectite layer percentages and transition probabilities of the I/S were determined according to Watanabe (1988). Many simulated XRD patterns were calculated as a function of K content in the illite interlayers, Fe content in the octahedral sheet, number of layers in the diffraction crystallite, and thickness of EG-smectite complex. Based upon the preliminary calculations, the K content of the illite interlayer appeared to be about 0.75 ions per illite half unit cell, the Fe contents of both the smectite and illite layers to be zero, the thickness of EG-smectite complex layer to be 16.9 Å, and the average number of layers in the diffracting crystallite to be 10 and to have a Gaussian distribution, except for sample A1. For sample A1, the average number of layers appeared to be 20. Thus, if such a variable was fixed, the % S and the transition probabilities in I/S were determined by trial and error methods, so that the relative intensity and position of all peaks in observed and calculated XRD patterns optimally agreed throughout the entire XRD pattern of each sample.

Table 3. Structure formulae (per half unit cell) of Kinnekulle illite/smectite samples.

Samples[1]	Method	Si (STD[2])	Al (STD[2])	Fe^{3+} (STD[2])	Mg (STD[2])	Ca (STD[2])	K (STD[2])	Na	Analyzed particles
STM6	AEM[3]	3.69 (±0.12)	1.71 (±0.08)	0.18 (±0.04)	0.60 (±0.02)	0.06 (±0.02)	0.27 (±0.05)	nd[6]	4
	wet[4]	3.80	1.66	0.16	0.41	—	0.25	0.33[7]	
B31	AEM[3]	3.64 (±0.12)	1.81 (±0.14)	0.14 (±0.02)	0.52 (±0.07)	0.07 (±0.02)	0.42 (±0.08)	nd[6]	6
	wet[4]	3.67	1.82	0.13	0.42	—	0.38	0.27[7]	
A2	AEM[3]	3.67 (±0.08)	1.86 (±0.08)	0.11 (±0.01)	0.45 (±0.07)	0.05 (±0.02)	0.38 (±0.07)	nd[6]	6
	wet[5]	3.77	1.74	0.11	0.41	—	0.40	0.14[7]	
K78	AEM[3]	3.47 (±0.14)	2.07 (±0.06)	0.17 (±0.10)	0.38 (±0.14)	0.06 (±0.01)	0.56 (±0.09)	nd[6]	7
	wet[4]	3.59	2.00	0.14	0.30	—	0.52	0.16[7]	

[1] See Table 1 for sample descriptions.
[2] Standard deviation.
[3] By analytical transmission electron microscope.
[4] Cited from Brusewitz (1986, 1988).
[5] Cited from Hower and Mowatt (1966).
[6] Not determined.
[7] Sum of exchangeable cations as a monovalent cation.

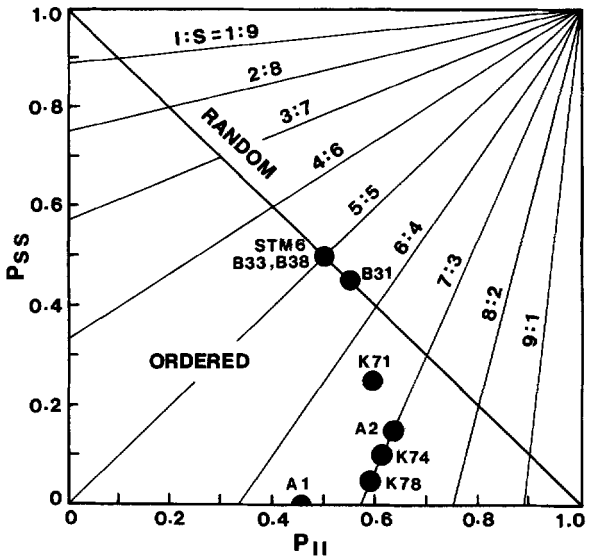

Figure 3. Plots of illite/smectite from Kinnekulle in the transition probabilities (P_{ss} and P_{II}) diagram.

RESULTS

Structure of I/S from Kinnekulle bentonites

Figure 2 compares the observed XRD patterns with the calculated patterns for Kinnekulle I/S samples. Small maxima on the observed patterns not present on the calculated patterns represent other minerals present in the samples, as shown in Table 1.

The XRD patterns of air-dried samples B31 and B33 showed weak maxima at about 3°2θ, indicating the presence of a large-spacing phase coexisting with 17-Å phase. Brusewitz (1986) suggested that these samples were a mixture of two types of I/S having g = 0 and g = 1 structures. In unpublished data from this laboratory, these materials gave a weak, large-spacing reflection only for the original, Ca-saturated, and Sr-saturated specimens in the air-dried state. This large-spacing reflection was not clearly present in the patterns of other cation-saturated specimens nor in those of the EG-saturated specimens (Figures 2a and 2b), suggesting that the amount of I/S having g = 1 structure was very small in samples B31 and B33. Samples K71, K74, and K78 were also considered to consist of two types of I/S having g = 0 and g = 1 structures (Brusewitz, 1986). They were composed chiefly of I/S having a g = 1 structure on the basis of a main 13-Å peak as a second-order reflection (Figures 2c, 2d, and 2e). Thus, the mixture effect of two types of I/S was not taken into account in the simulations of XRD patterns on the Kinnekulle samples. The above approximations led to somewhat large disagreement in peak position, particularly in the $(001)_{10}/(002)_{17}$ peak, between the observed and calculated XRD patterns, as shown in Figure 2. They also led to differences in the % S values (P_S values in Table 2) from those reported previously, although the previous % S data were estimated by different techniques. Despite these facts, the % S values and transition probabilities determined in this study (Table 2) probably represent a main part of interstratified structures in each sample.

All the Kinnekulle samples approximately consisted of either g = 0 or g = 1 structures. Thus, the following relation exists between the existence probabilities (P_I and P_S) and the transition probabilities (P_{II} and P_{SS}): $P_{SS} = K \cdot P_{II} + (1 - K)$ and $K = P_I/P_S$ (Sato, 1965), where P_I and P_S indicate the existence probabilities of illite and smectite layers within a stacking arrangement, and P_{II} and P_{SS} are the transition probabilities from illite layer to illite layer and from smectite layer to smectite layer, respectively. Sato (1965) and Sato and Kizaki (1972) applied this relation to a classification of I/S as shown in Figure 3. Randomly interstratified I/S falls along the diagonal tied from a pole (0, 1) to another pole (1, 0) of (P_{II}, P_{SS}) in the figure. Plots above the diagonal represent segregation structures of I/S and those below the diagonal represent short-range ordered (g = 1) structures. Samples STM6, B31, B33, and B38 fall along the diagonal. The other samples scatter with variable P_{SS} values in the field of short-range ordered structures.

All of the Kinnekulle I/S showed no clear *hkl* reflections in the range 19–36°2θ, as was observed by Brusewitz (1986); hence, the basic structure of the I/S, such as its polytype, could not be specified. This is quite different from I/S having the same % S from hydrothermally altered tuffs; this material displayed characteristic *hkl* reflections indicating 1*M* symmetry (Inoue *et al.*, 1987).

Morphology

Figure 4 shows TEM photographs of Kinnekulle samples. All the I/S samples are composed chiefly of dominantly flaky particles and small amounts of laths. Drastic differences in morphology were not observed in the range 30–50% S. The average length/width ratio of the lath particles is about 4, regardless of % S, based upon measurement of about 30 particles in each sample, although some ratios were great as 20 (Figure 4e). Such aspect ratios of laths are quite different from those of the I/S from hydrothermally altered tuffs (8–9 for 50% S and 10 for 30% S) (Inoue *et al.*, 1988).

As estimated from Pt-Pd shadowing, the thickness of the I/S particles in the Kinnekulle samples ranged

→

Figure 4. Transmission electron microphotographs of (a, b) sample STM6, (c, d) sample A2, and (e, f) sample K78 shadowed with Pt-Pd. Bars represent 0.1 μm.

https://doi.org/10.1346/CCMN.1990.0380302 Published online by Cambridge University Press

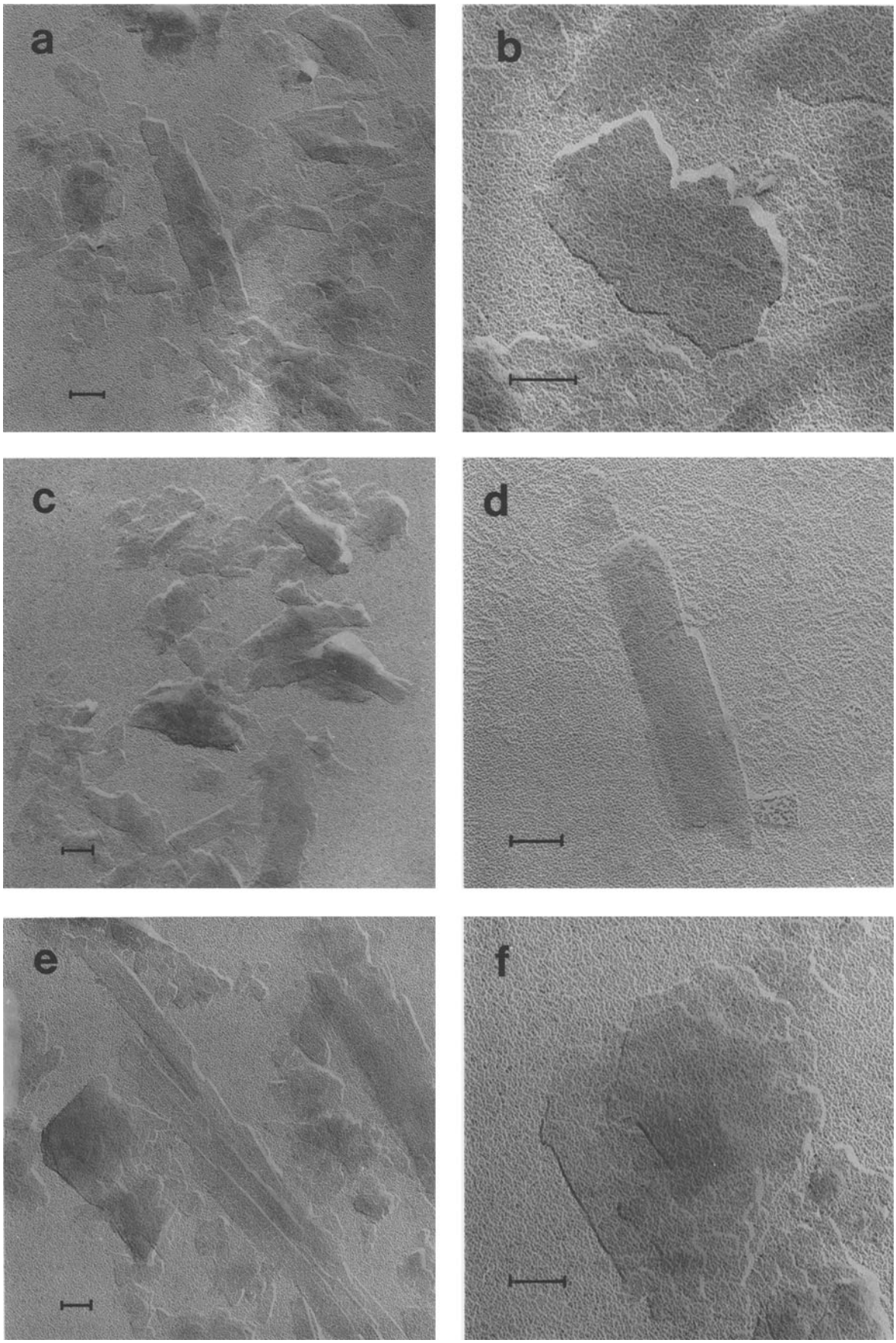

https://doi.org/10.1346/CCMN.1990.0380302 Published online by Cambridge University Press

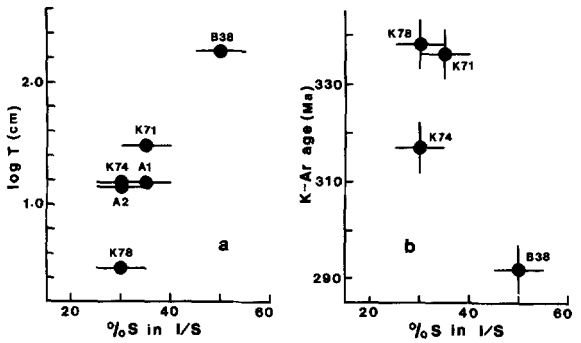

Figure 5. Relationships of percentage of smectite layers and (a) logarithmic thickness of bentonite beds and (b) K-Ar age in the Kinnekulle bentonites.

from 30 to 100 Å (Figure 4). Nadeau *et al.* (1984), however, reported that bentonite samples, sample CCB (50% S) and sample SFB (25% S), contained a range of particle thickness from 10 to 50 Å and from 20 to 50 Å, respectively. Inoue *et al.* (1987) reported that hydrothermal samples [sample H (50% S) and sample M (20% S)] contained a range of particle thickness from 20 to 40 Å and from 30 to 60 Å, respectively. Although the thicknesses were dependent on the sample preparation technique, as noticed by Ahn and Peacor (1986), the thickness of Kinnekulle I/S particles was found to be nearly equivalent to the values reported by Nadeau *et al.* (1984, 1985) and Inoue *et al.* (1987). No systematic variation in the thickness of I/S particles was detected with decreasing % S in the range 30–50% S.

Chemical composition

Table 3 gives the chemical composition of Kinnekulle I/S as determined by the present AEM technique, as well as from data determined previously by wet chemical methods (Hower and Mowatt, 1966; Brusewitz, 1986, 1988). The compositions are similar except for the Ca and Fe contents. The analyses indicate that the K and Al contents of the I/S increase and the Si and Mg contents decreased continuously with decreasing % S. No significant difference in chemical composition was detected between particles of different shapes.

Relations between % S and thickness of bentonite beds, and K-Ar age in I/S

The % S in the Kinnekulle I/S could not be related to the position of bentonite beds in the geological column shown in Figure 1. The relations between the % S and thickness of each bed, and the K-Ar age in the Kinnekulle I/S seem to be significant (Figure 5). Sample B38 from the thick B bed is representative of the bed because it was collected from the central part of the bed (Figure 1). Figure 5 apparently indicates that the % S in the I/S is smaller in thin beds than in thick beds. Less expandable I/S generally gave an older K-Ar age. Apparently, the illitization of smectite progressed to a greater extent in thinner beds and it took place at an earlier time. Velde and Brusewitz (1982) and Brusewitz (1986, 1988) indicated a zonal distribution of % S and K, Rb, and Sr contents in I/S within the thick B bed. They attributed the zonal distribution to a diffusion process through the bentonite during diagenesis. Similar diffusion processes attending I/S formation were described for a bentonite from the Montana disturbed belt by Altaner *et al.* (1984) and Altaner (1989).

DISCUSSION

If the diffusion process mentioned above is valid for the formation of I/S at Kinnekulle, the present experimental results characterize the smectite-to-illite conversion in bentonites due to the metasomatic and dia-

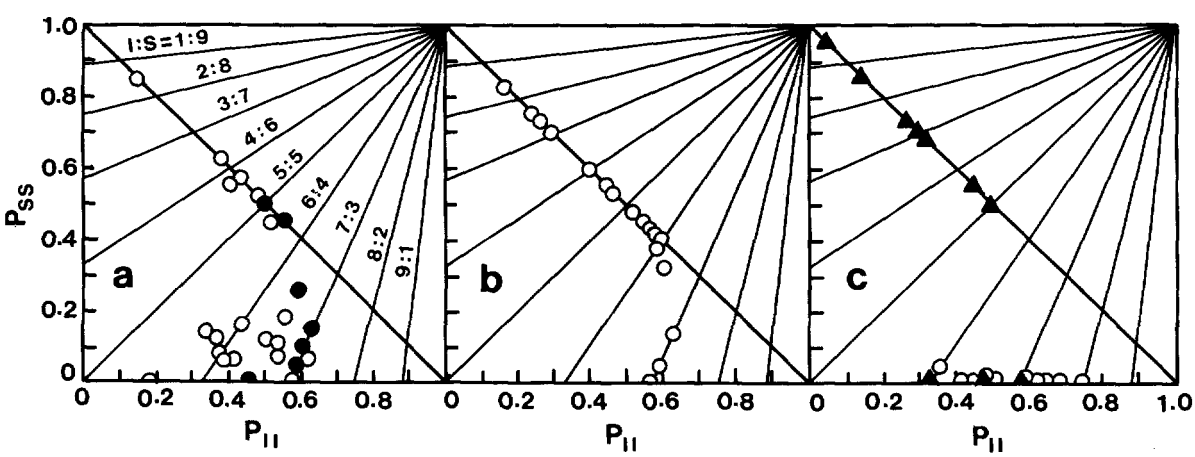

Figure 6. Plots of illite/smectite from various origins in transition probabilities (P_{SS} and P_{11}) diagram: (a) illite/smectite from bentonites by Bethke *et al.* (1986) (○), including Kinnekulle samples (●); (b) illite/smectite from shales by Bethke *et al.* (1986) (○); and (c) illite/smectite from hydrothermally altered tuffs by Bethke *et al.* (1986) (○), including Shinzan samples by Inoue *et al.* (1987) (▲).

https://doi.org/10.1346/CCMN.1990.0380302 Published online by Cambridge University Press

genetic processes as follows: (1) The structure of I/S changes gradually and continuously from random (g = 0) to ordered (g = 1), accompanying a continuous change in transition probability from $P_{SS} > 0$ to $P_{SS} = 0$. (2) The morphology of I/S particles does not change drastically with the structure change. (3) Elemental substitutions proceed continuously with the structure change. A drastic change in morphology of I/S particles from hydrothermally altered tuffs suggests that smectite layers dissolve and recrystallize as illite layers during the smectite-to-illite conversion, as mentioned above. At Kinnekulle, on the other hand, the % S of the I/S decreased with no drastic morphological change, suggesting that distinct dissolution and recrystallization of I/S grains did not occur during the smectite-to-illite conversion (at least in the range of 50% S to 30% S) during diagenesis. Of the suitable mechanisms for the smectite-to-illite conversion at Kinnekulle described above, the solid-state transformation mechanism explains more reasonably all these observations.

Figure 6 compares the interlayer structures of I/S from various types of rocks on the P_{II}-P_{SS} diagram. All I/S phases containing 100–50% S, regardless of origin, plot on the line, indicating random structure. Random interstratification is apparent for samples containing <40% S for I/S phases from the bentonites and shales (Figures 6a and 6b). With decreasing % S, the I/S from hydrothermally altered tuffs changes abruptly to an ordered structure, containing about $P_{SS} = 0$. This peculiar behavior was pointed out by Inoue and Utada (1983), who indicated that some I/S samples would plot between g = 0 and g = 1 curves in the $\Delta 2\theta_1$-$\Delta 2\theta_2$ diagram of Watanabe (1981). On the other hand, the I/S from the shales and bentonites changes from an ordered structure (g = 1), with $P_{SS} > 0$, to a structure (g = 1) with $P_{SS} = 0$, as P_{SS} gradually decreases towards zero. The different modes of structural transformation in various types of rocks may be related to the porosity and permeability of rocks rather than to the origin of I/S, (e.g., diagenesis and hydrothermal deposition). Only a few structure analyses have been made on I/S from sandstones and shales having high porosity and permeability. Grain morphology of I/S, however, was described by Glasmann *et al.* (1989) for lath-shaped I/S in shales having high porosity during diagenesis. Many published TEMs of I/S (Güven *et al.*, 1980; Hugget, 1982; McHardy *et al.*, 1982; Nadeau *et al.*, 1985) indicate that I/S in sandstones occurs as laths or filaments and that I/S in bentonites occurs dominantly as flakes, similar to those of the Kinnekulle samples. Euhedral lath-shaped I/S is found predominantly in rocks having high porosity, such as hydrothermally altered tuffs and sandstones, which apparently provided spaces so that the I/S crystals could grow freely. In rocks having low porosity, such as shales and bentonites, few open spaces existed, and solution did not circulate freely. Thus, the elements which were necessary to form illite layers would not have been supplied in sufficient quantity during the smectite-to-illite conversion in rocks having low porosity and permeability. The limited supply of elements probably controlled the degree of illitization of the smectite. The abrupt transformation from $P_{SS} > 0$ to $P_{SS} = 0$ structures in I/S was probably intimately related to the morphological change in the I/S particles (Inoue *et al.*, 1987). Consequently, the porosity and permeability of the original rocks significantly influenced the morphology of I/S particles, the degree of illitization, the mode of structure transformation, and, as a whole, the mechanism of the smectite-to-illite conversion. This conclusion can be applied to the smectite-to-illite conversion in the range 100–30% S, taking into account the % S range studied here.

ACKNOWLEDGMENTS

The authors are indebted to B. Velde for helpful reviews of an initial version of the manuscript.

REFERENCES

Ahn, J. H. and Peacor, D. R. (1986) Transmission and analytical electron microscopy of the smectite-to-illite transition: *Clays & Clay Minerals* **34,** 165–179.

Altaner, S. P. (1989) Calculation of K diffusional rates in bentonite beds: *Geochim. Cosmochim. Acta* **53,** 923–931.

Altaner, S. P., Hower, J., Whitney, G., and Aronson, J. L. (1984) Model for K-bentonite formation: Evidence from zoned K-bentonites in the disturbed belt, Montana: *Geology* **12,** 412–415.

Bethke, C. M., Vergo, N., and Altaner, S. P. (1986) Pathways of smectite illitization: *Clays & Clay Minerals* **34,** 125–135.

Boles, J. R. and Franks, S. G. (1979) Clay diagenesis in Wilcox sandstones of southwest Texas: Implications of smectite diagenesis on sandstone cementation: *J. Sed. Petrol.* **49,** 55–70.

Brusewitz, A. M. (1984) Preliminary report on potassium bentonites in Sweden. A study of illite-smectite minerals: in *Smectite Alteration,* D. M. Andersson, compiler, *Swedish Nuclear Fuel and Waste Management Co. Tech. Rept.* **84-11,** 105–121.

Brusewitz, A. M. (1986) Chemical and physical properties of Paleozoic potassium bentonites from Kinnekulle, Sweden: *Clays & Clay Minerals* **34,** 442–454.

Brusewitz, A. M. (1988) Asymmetric zonation of a thick Ordovician K-bentonite bed at Kinnekulle, Sweden: *Clays & Clay Minerals* **36,** 349–353.

Eberl, D. D. and Hower, J. (1976) Kinetics of illite formation: *Geol. Soc. Amer. Bull.* **87,** 1326–1330.

Eberl, D. D. and Środoń, J. (1988) Ostwald ripening and interparticle-diffraction effects for illite crystals: *Amer. Mineral.* **73,** 1335–1345.

Glasmann, J. R., Larter, S., Briedis, N. A., and Lundegard, P. D. (1989) Shale diagenesis in the Bergen high area, North Sea: *Clays & Clay Minerals* **37,** 97–112.

Güven, N., Hower, W. F., and Davies, D. K. (1980) Nature of authigenic illites in sandstone reservoirs: *J. Sed. Petrol.* **50,** 761–766.

Hoffman, J. and Hower, J. (1979) Clay mineral assemblages as low grade metamorphic geothermometers: Application to the thrust faulted disturbed belt of Montana, U.S.A.: *Soc. Econ. Paleontol. Mineral. Spec. Publ.* **26,** 55–79.

Horton, D. G. (1985) Mixed-layer illite/smectite as a paleotemperature indicator in the Amethyst vein system, Creede district, Colorado, USA: *Contrib. Mineral. Petrol.* **91,** 171–179.

Hower, J. (1981) Shale diagenesis: in *Clays and the Resource Geologist,* F. J. Longstaff, ed., *Short Course Handbook 7,* Mineral. Assoc. Canada, 60–80.

Hower, J., Eslinger, E., Hower, M., and Perry, E. (1976) The mechanism of burial diagenesis reaction in argillaceous sediments, 1. Mineralogical and chemical evidence: *Geol. Soc. Amer. Bull.* **87,** 725–737.

Hower, J. and Mowatt, T. C. (1966) The mineralogy of illite and mixed-layer illite-montmorillonites: *Amer. Mineral.* **51,** 825–854.

Hugget, J. M. (1982) On the nature of fibrous illite as observed by electron microscope: *Clay Miner.* **17,** 433–441.

Inoue, A., Bouchet, A., Velde, B., and Meunier, A. (1989) Convenient technique for estimating smectite layer percentage in randomly interstratified illite/smectite minerals: *Clays & Clay Minerals* **37,** 227–234.

Inoue, A., Kohyama, N., Kitagawa, R., and Watanabe, T. (1987) Chemical and morphological evidence for the conversion of smectite to illite: *Clays & Clay Minerals* **35,** 111–120.

Inoue, A. and Utada, M. (1983) Further investigations of a conversion series of dioctahedral mica/smectites in the Shinzan hydrothermal alteration area, northeast Japan: *Clays & Clay Minerals* **31,** 401–412.

Inoue, A., Velde, B., Meunier, A., and Touchard, G. (1988) Mechanism of illite formation during smectite-to-illite conversion in a hydrothermal system: *Amer. Mineral.* **73,** 1325–1334.

Jagodzinski, H. (1949) Eindimensionale Fehlordnung in Kristallen und ihr Einfluss auf die Röntgeninterferenzen. I. Berechnung des Fehlordnungsgrades aus der Rontgenintensitaten: *Acta Crystallogr.* **2,** 201–207.

McHardy, W. J., Wilson, M. J., and Tait, J. M. (1982) Electron microscope and X-ray diffraction studies of filamentous illitic clay from sandstones of the Magnus Field: *Clay Miner.* **17,** 23–39.

Nadeau, P. H., Tait, J. M., McHardy, W. J., and Wilson, M. J. (1984) Interstratified XRD characteristics of physical mixtures of elementary clay particles: *Clay Miner.* **19,** 67–76.

Nadeau, P. H., Wilson, M. J., McHardy, W. J., and Tait, J. M. (1985) The conversion of smectite to illite during diagenesis: Evidence from some illitic clays from bentonites and sandstones: *Mineral. Mag.* **49,** 393–400.

Pollard, C. O. (1971) Semidisplacive mechanism for diagenetic alteration of montmorillonite layers to illite layers: *Geol. Soc. Amer. Spec. Paper* **134,** 79–93.

Pollastro, R. M. (1985) Mineralogical and morphological evidence for the formation of illite at the expense of illite/smectite: *Clays & Clay Minerals* **33,** 265–274.

Ramseyer, K. and Boles, J. R. (1986) Mixed-layer illite/smectite minerals in Tertiary sandstones and shales, San Joaquin basin, California: *Clays & Clay Minerals* **34,** 115–124.

Reynolds, R. C. and Hower, J. (1970) The nature of interlayering in mixed-layer illite-montmorillonites: *Clays & Clay Minerals* **18,** 25–36.

Roberson, H. E. and Lahann, R. W. (1981) Smectite to illite conversion rates, effects of solution chemistry: *Clays & Clay Minerals* **29,** 129–135.

Sato, M. (1965) Structure of interstratified minerals: *Nature* **208,** 70–71.

Sato, M. and Kizaki, Y. (1972) Structure of a 38 Å interstratified mineral, an illite-montmorillonite mixture: *Z. Kristallogr.* **135,** 219–231.

Środoń, J. and Eberl, D. D. (1984) Illite: in *Micas, Reviews in Mineralogy 13,* S. W. Bailey, ed., Mineral. Soc. Amer., Washington, D.C., 495–544.

Velde, B. and Brusewitz, A. M. (1982) Metasomatic and non-metasomatic low grade metamorphism of Ordovician metabentonites in Sweden: *Geochim. Cosmochim. Acta* **46,** 447–452.

Watanabe, T. (1981) Identification of illite/montmorillonite interstratification by X-ray powder diffraction: *J. Mineral. Soc. Japan, Spec. Issue* **15,** 32–41 (in Japanese).

Watanabe, T. (1988) The structural model of illite/smectite interstratified minerals and the diagram for its identification: *Clay Sci.* **7,** 97–114.

Yau, Y.-C., Peacor, D. R., and McDowell, S. D. (1987) Smectite-to-illite reactions in Salton Sea shales: A transmission and analytical electron microscope study: *J. Sed. Petrol.* **57,** 335–342.

(Received 27 July 1989; accepted 4 December 1989; Ms. 1936)